International Journal of Engineering Research & Technology (IJERT)
ISSN: 2278-0181
Vol. 3 Issue 10, October- 2014

Computation of Flow and Temperature Distribution in Ventilated Enclosure with Uniform Heating of Top Wall

Robins Aikkara
Dept. of Mechanical Engineering
LBS College of Engineering
Kasaragod, India

Aboobacker Kadengal
Dept. of Mechanical Engineering
LBS College of Engineering
Kasaragod, India

***Abstract*— Combined free convection and forced convection from a uniform heat source on the top wall of a enclosure with inlet and outlet opening is studied numerically. Two-dimensional forms of non-dimensional Navier-Stokes equations are solved by using control volume based finite volume technique. Three typical values of the Reynolds numbers are chosen as Re = 1, 10, and 100 and steady, laminar results are obtained in the values of Richardson number as Ri = 0, 1 and 10 and the values of Prandtl numbers as Pr = 0.1, 0.71, 1 and 10. The parametric studies for a wide range of governing parameters show consistent performance of the present numerical approach to obtain as stream functions and temperature profiles. Heat transfer rates at the heated walls are presented based on the value of Re and Pr. The computational results indicate that the heat transfer is strongly affected by Reynolds number and Richardson number. In the present investigation, bottom wall is uniformly heated while the two vertical walls are maintained at constant cold temperature and the top wall is well insulated. A complete study on the effect of Ri shows that the strength of circulation increases with the increase in the value of Ri irrespective of Re and Pr. As the value of Ri increases, there occurs a transition from conduction to convection dominated flow at Ri =1. A detailed analysis of flow pattern shows that the natural or forced convection is based on both the parameters Ri and Pr.**

Keywords— Mixed convection; Ventilated enclosure; Uniform heating; Reynolds number; Richardson number and Prandtl number.

I. INTRODUCTION

Thermal buoyancy forces play a significant role in forced convection heat transfer when the flow velocity is relatively small and the temperature difference between the surface and the free stream is relatively large. The buoyancy force modifies the flow and the temperature fields and hence the heat transfer rate from the surface. Problems of heat transfer in enclosures by free convection or combined free and forced convection have been the subject of investigations for many years. Mixed convection occurs in many heat transfer devices, such as the cooling system of a nuclear power plant, large heat exchangers, cooling of electronic equipment, ventilation and heat or pollution agent clearance. The relative direction between the buoyancy force and the externally forced flow is important.

Since the early work by Burggraf [1], the lid-driven cavity flow is considered as the classical test problem for the assessment of numerical methods and the validation of Navier-Stokes codes. Highly-accurate solutions for the lid-driven cavity flow are computed by a Chebyshev collocation method is done by O. Botella [2]. Accuracy of the solution is achieved by using a subtraction method of the leading terms of the asymptotic expansion of the solution of the Navier-Stokes equations in the vicinity of the corners, where the velocity is discontinuous. Critical comparison with former numerical experiments confirms the high-accuracy of the method, and extensive results for the flow at Reynolds number Re = 1000 are presented. The Charles-Henri Bruneau [3], numerically simulate of the 2D lid-driven cavity flow are performed for a wide range of Reynolds numbers. Accurate benchmark results are provided for steady solutions as well as for periodic solutions around the critical Reynolds number.

In the present investigation, top wall is uniformly heated while the two vertical walls are maintained at constant cold temperature and the bottom wall is well insulated. The inlet opening is located at the top of left vertical wall and out let opening is located at bottom of right vertical wall. A complete study on the effect of Gr shows that the strength of circulation increases with the increase in the value of Ri irrespective of Re and Pr. As the value of Ri increases, there occurs a transition from conduction to convection dominated flow. A detailed analysis of flow pattern shows that the natural or forced convection is based on both the parameters Ri and Pr.

II. MATHEMATICAL FORMULATION

A two-dimensional ventilated enclosure is considered for the present study with the physical dimension as shown in Fig.1. The ventilated square enclosure with constant wall temperature heat source embedded on the top wall; inlet opening located on the top of left vertical wall; and outlet opening on the bottom of right vertical wall. The depth of the ventilated enclosure is presumed to be infinitely long so that the whole model is two-dimensional. For simplicity, the height of the two openings is kept same and equal to half

of vertical walls. The bottom wall of the enclosure is taken as adiabatic. The flow velocity of the fluid through the inflow opening are assumed to be uniform (U^0) at constant temperature T_c. The flow is assumed to be laminar and the fluid properties are assumed to be constant except for the density variation which is modeled according to Boussinesq approximation while viscous dissipation effects are considered to be negligible. The viscous incompressible flow and the temperature distribution inside the cavity are governed by the Navier–Stokes and the energy equations, respectively. The aim of the current work is to investigate the steady state solutions and hence, we have considered the time independent differential governing equations. Similar procedure was also followed in the recent work on mixed convection. A number of earlier works was based on steady state solutions which were obtained via steady mathematical model. The governing equations are non-dimensionalized to yield

$$\frac{\partial U}{\partial X}+\frac{\partial V}{\partial Y}=0 \quad (1)$$

$$U\frac{\partial U}{\partial X}+V\frac{\partial U}{\partial Y}=-\frac{\partial P}{\partial X}+\frac{1}{Re}\left(\frac{\partial^2 U}{\partial X^2}+\frac{\partial^2 U}{\partial Y^2}\right) \quad (2)$$

$$U\frac{\partial V}{\partial X}+V\frac{\partial V}{\partial Y}=-\frac{\partial P}{\partial Y}+\frac{1}{Re}\left(\frac{\partial^2 V}{\partial X^2}+\frac{\partial^2 V}{\partial Y^2}\right)+\frac{Gr}{Re^2}\theta \quad (3)$$

$$U\frac{\partial \theta}{\partial X}+V\frac{\partial \theta}{\partial Y}=\frac{1}{RePr}\left(\frac{\partial^2 \theta}{\partial X^2}+\frac{\partial^2 \theta}{\partial Y^2}\right) \quad (4)$$

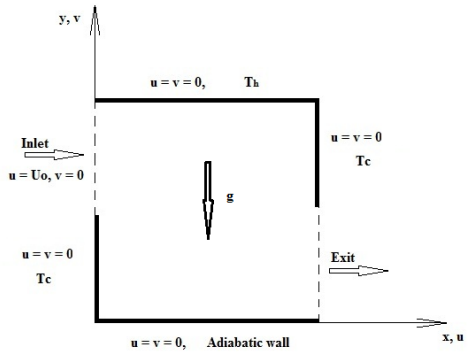

Fig.1. Schematic diagram of a physical system

The transformed boundary conditions are:

U (X, 1) = 1,
U (X, 0) = U (0, Y) = U (1, Y) = 0
V (X, 0) = V (X, 1) = V (0, Y) = V (1, Y) = 0
θ (X, 0) = 1
θ (0, Y) =θ (1, Y) = 0
$\frac{\partial \theta}{\partial Y}(X,1)=0$

The dimensionless variables and parameters are defined as follows:

$$X=\frac{x}{L},\quad Y=\frac{y}{L},\quad U=\frac{u}{U_0}$$
$$V=\frac{v}{V_0},\quad \theta=\frac{T-T_c}{T_h-T_c},\quad P=\frac{p}{\rho U_0^2}$$
$$Pr=\frac{\nu}{\alpha},\quad Re=\frac{U_0 L}{\nu},\quad Gr=\frac{g\beta(T_h-T_c)L^3}{\nu^2}$$

Here x and y are the distances measured along the horizontal and vertical directions, respectively; u and v are the velocity components in x and y directions, respectively; T denotes the temperature; p is the pressure and ρ is the density; T_h and T_c are the temperature at the hot and cold walls, respectively; L is the length of the side of the ventilated cavity; X and Y are dimensionless coordinates varying along horizontal and vertical directions, respectively; U_0 is the velocity of the upper wall; U and V are dimensionless velocity components in the X and Y directions, respectively; θ is the dimensionless temperature; P is the dimensionless pressure; Gr, Re and Pr are Grashof, Reynolds and Prandtl number, respectively.

III. SOLUTION METHODOLOGY

The momentum and energy balance equations [Eqs. (2) – (4)] are the combinations of a system of equations which have been solved using the finite volume method. The continuity equation [Eq. (1)] has been used as a constraint due to mass conservation and this constraint may be used to obtain the pressure distribution. In order to solve Eqs. (2) – (3), we use the finite volume discretisation procedure, if the nonlinearity in the momentum equations appears to be a difficulty in iteration procedure. Starting with a guessed velocity field, we could iteratively solve the momentum equations to arrive at the converged solution for the velocity components. The real difficulty in the calculation of the velocity field lies in the unknown pressure field. The pressure gradient forms a part of the source term for a momentum equation. For a given pressure field, there is no particular difficulty in solving the momentum equation. The pressure field is indirectly specified via the continuity equation [Eq. (1)]. When the correct pressure field is substituted into the momentum equations, the resulting velocity field satisfies the continuity equation.

The discretised form of X-momentum [Eq. (2)] is written as

$$a_e U_e=\sum a_{nb}U_{nb}+b+(P_p-P_E)A_e \quad (5)$$

where $A_e = \Delta Y$

The discretised form of Y-momentum [Eq. (3)] is written as

$$a_n V_n=\sum a_{nb}V_{nb}+b+(P_p-P_N)A_n \quad (6)$$

where $A_n = \Delta X$.

The momentum equations can be solved only when the pressure field is given. Unless the correct pressure field is employed the resulting velocity field will not satisfy the continuity equations. Such an imperfect velocity field based on a guessed pressure field P^* will be denoted by U^*, V^*. This "starred" velocity field will result from the solution of the following discretisation equations:

$$a_e U^*_e=\sum a_{nb}U^*_{nb}+b+(P^*_p-P^*_E)A_e \quad (7)$$

$$a_n V^*_n=\sum a_{nb}V^*_{nb}+b+(P^*_p-P^*_N)A_n \quad (8)$$

In these equations [Eq. (7), (8)], the velocity components and pressure have been given the superscript *.

The guessed pressure P^* and resulting starred velocity field will progressively get closer to satisfying the

continuity equation. Let us propose that the correct pressure P is obtained from

$$P = P^* + P' \quad (9)$$

where P' will be called the pressure correction. The corresponding velocity corrections U', V' can be introduced in a similar manner:

$$U = U^* + U', \qquad V = V^* + V' \quad (10)$$

The equation (12) will be used to correct the momentum equations:

$$U_e = U_e^* + d_e(P_P' - P_E') \quad (11)$$

$$V_n = V_n^* + d_n(P_P' - P_N') \quad (12)$$

The computational procedure is similar to the one described by Baliga and Patankar (1983), and Gresho et al. (1984). The resulting system of the coupled equations (1-4) with the associated boundary conditions have been solved numerically using control volume based finite volume method. The computational domain consists of 50×50 main grid points which correspond to 50×40 U and V staggered grid points. The control volume based finite volume method provides the smooth solutions at the interior domain including the corner regions. To ensure the convergence of the numerical solution to the exact solution, the grid sizes have been optimized and the results presented here are independent of grid sizes.

Grid refinement tests have been performed for the case Re = 100 and Gr = 1000 using eight uniform grids 15×15, 25×25, 40×40, 50×50, 60×60, 75×75, 90×90 and 100×100. Results show that when we change the mesh size from a grid of 25×25to a grid of 50× 50, the maximum value of stream function contour (ψ_{max}) and the maximum temperature contour (θ_{max}) undergoes an increase of only 0.5% and 0.25%, respectively; then, because of calculation cost, the 50×50 grid is retained.

The computer code has been validated with the solutions are available in the literatures. There are some possibilities of validating the numerical code. One possibility is to compare the numerical results obtained by our code with benchmarks available in the literature according to different works. Another option is to simulate a similar problem investigated by other authors with well accepted available results.

IV. RESULT AND DISCUSSION

The computational domain consists of 50×50 main grid points which correspond to 50×40 U and V staggered grid points. Numerical solutions are obtained for various values of Ri = 0 - 10, Pr = 0.01–10 and Re = 1–10^2 with uniform heating of the top wall where the two vertical walls are cooled and the inflow opening is located at the top of the left vertical wall with a horizontal velocity, U=1, and outflow opening is located at the bottom of right vertical wall. The jump discontinuity in Dirichlet type of wall boundary conditions at the corner point (see Fig.1) corresponds to computational singularity. To ensure the convergence of the numerical solution to the exact solution, the grid sizes have been optimized and the results presented here are independent of grid sizes.

A. *Characteristics of flow velocity*

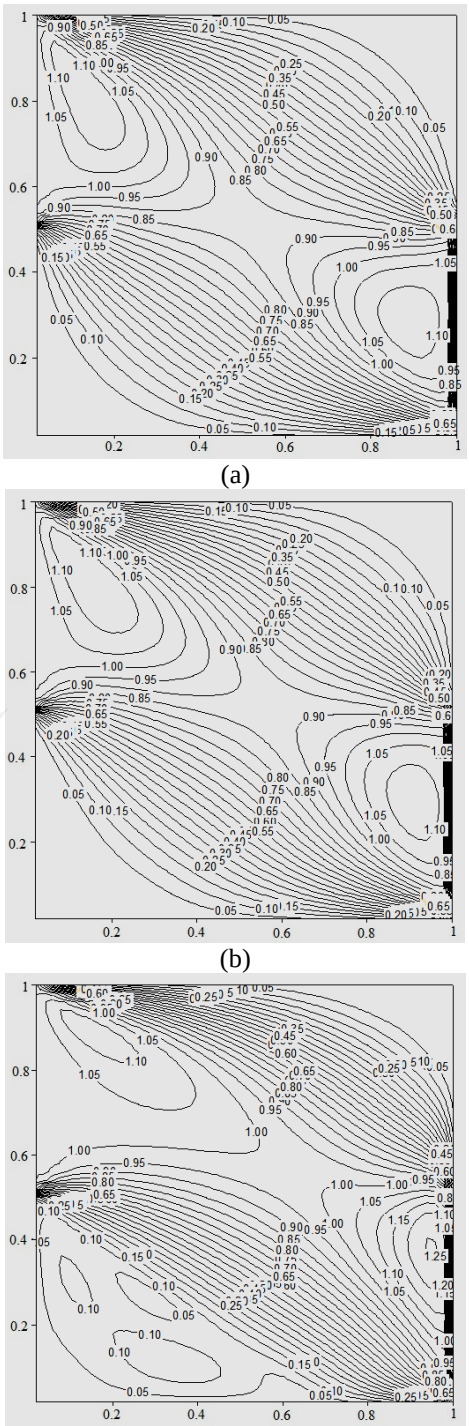

(a) (b) (c)

Fig.2. Flow velocity contours with Pr = 0.7, Ri =1: (a) Re = 1, (b) Re = 10, and (c) Re = 100

The Fig.2 (a)-(c) illustrate the velocity contours with the constant temperature heated top wall for Ri = 1, Pr = 0.7 and Re = 1 to 100. Fig.2 (a) show the effect of laminar flow, because it's and Re = 1. The velocity contours are distributed symmetrically about the diagonal wise. In the case of inflow

opening velocity contours are distributed in oval shape and outflow opening it is almost round shape. But in the case of Fig.2 (b), (c) the value of Re increases the shape of velocity contours will be changed. As the Re increases the velocity contours shifted in the top wall of the flow enclosure. In this case shape velocity contours at inlet and outlet opening are changed. Further increases in the value of Re circulating flow will be developed in the left bottom corner. The circulation in the left bottom corner will be stronger than that of right top corner.

B. Effect of Richardson number

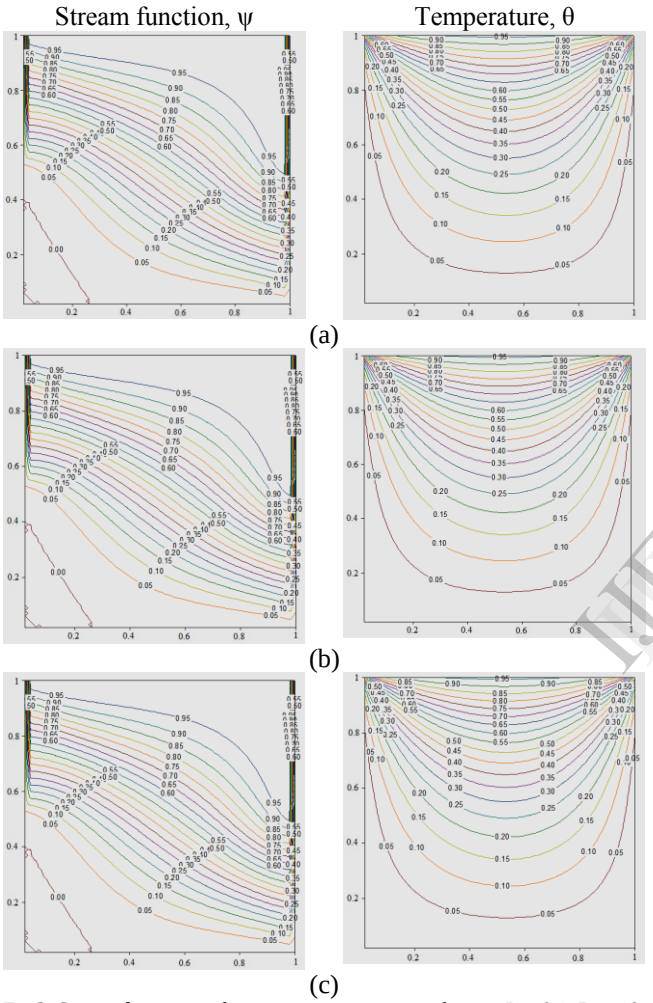

Fig.3. Stream function and temperature contours with Pr =0.1, Re =10: (a) Ri =0, (b) Ri =1, and (c) Ri =10

In order to understand the effect of Richardson number on the viscous flow and heat transfer phenomena, a parametric study of Ri varying from 0 to 10 is carried out. Three kinds of heat transfer regimes are observed according to the magnitude of Ri: a forced-convection dominated regime, a mixed-convection regime, and a buoyancy-dominated (or natural convection) regime. Figures 3–5 illustrate streamline and isotherm contours with the uniformly heated top wall for Ri at Re = 10 and Pr = 0.1 – 10. Fig.3 (a) show the effect of cavity flow predominates the Low Reynolds number forced convection with Ri =0 and Pr = 0.1. At very low values of Richardson number, such as 0 and 0.1, the forced convection due to the driven force dominates the flow structure. At this order of Ri, the inertia force of the fluid is dominant compared to the buoyancy force.

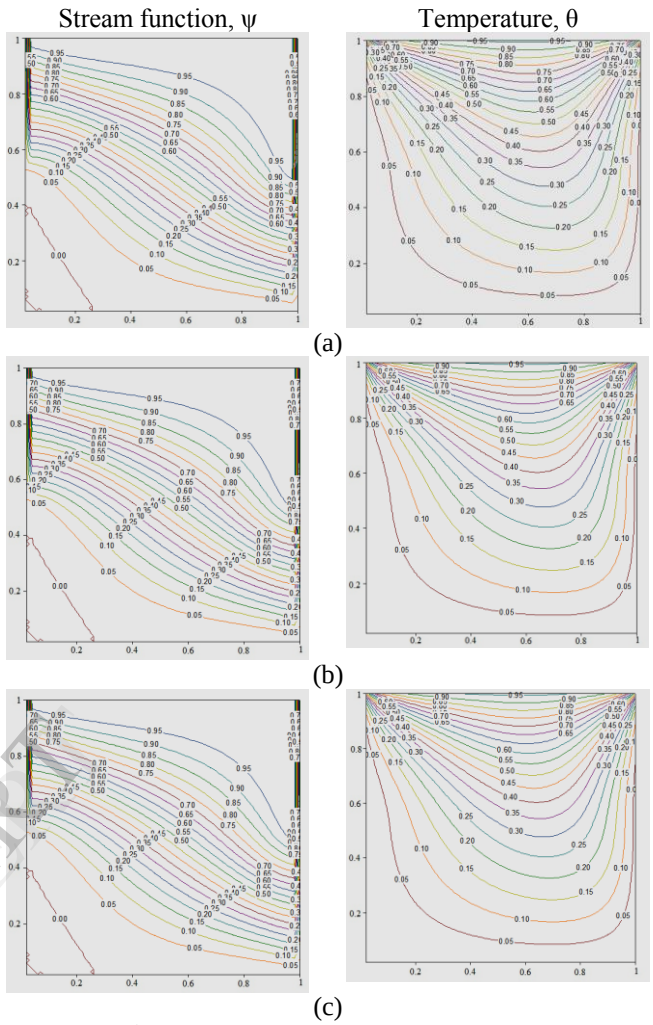

Fig.4. Stream function and temperature contours with Pr =0.7, Re =1: (a) Ri =0, (b) Ri =1, and (c) Ri =10

As the Richardson number increases to Ri = 1, the inertia and buoyancy forces balance each other, which then results in a mixed convection. When the Richardson number further increases to Ri= 10, the buoyancy force becomes the dominant mechanism to drive the convection of the fluid, and the flow is in the regime of natural convection.

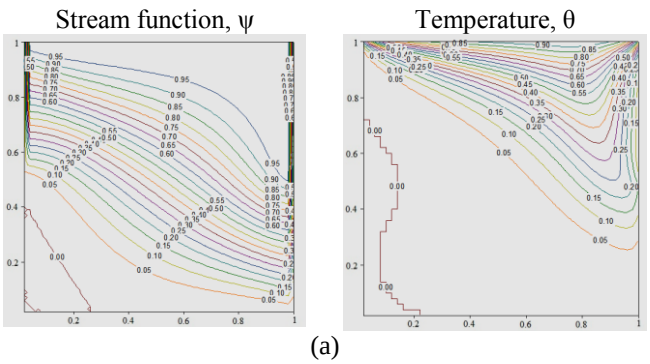

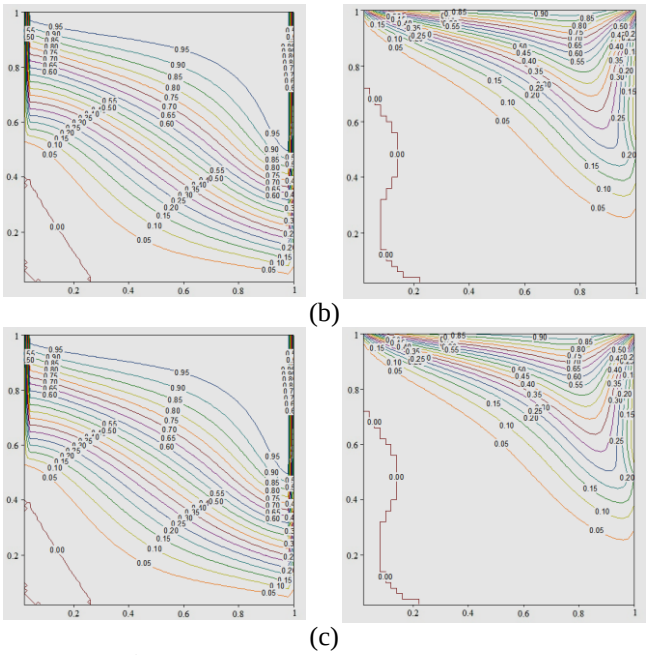

Fig.5. Stream function and temperature contours with Pr =10, Re =1: (a) Ri =0, (b) Ri =1, and (c) Ri =10

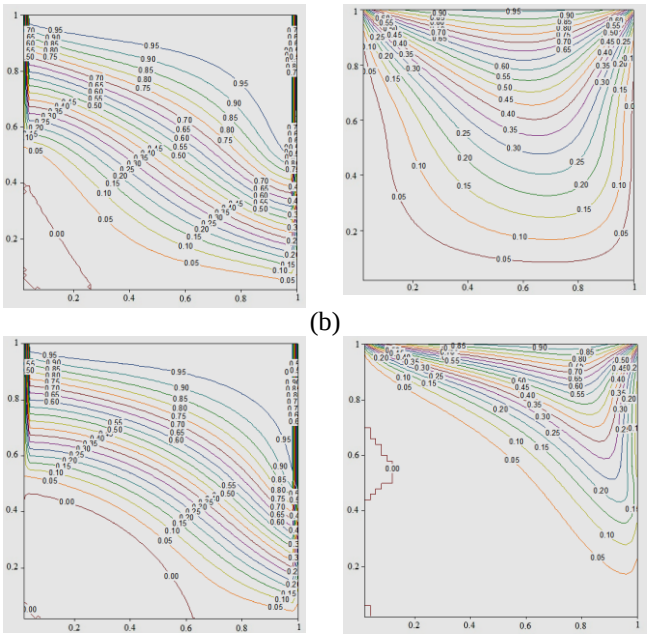

Fig.6. Stream function and temperature contours with Pr = 0.7, Ri =1: (a) Re =1, (b) Re =10, (c) Re =10^2

The Fig. 3 shows the temperature contours are smooth symmetric curves that span the entire cavity. But in the case of Fig. 4 and 5 the larger value of Pr and hence the isotherms gradually tend to be asymmetric. The value of Prandtl number Pr up to 10 the isotherms are shifted to right wall of the cavity; then the cold region will be developed in the side of left wall.

C. Effect of Reynolds number

The characteristics of the mixed convection phenomenon can be well understood by plotting the streamlines for various Reynolds number as shown in Fig. 6 and 7. For all values of Re, the stream line patterns inside the enclosure is found to vary with Ri in a regular fashion as expected within the laminar regime. Fig. 6 shows the effect of mixed convection flow in a ventilated enclosure with different Re values with Ri = 1 and Pr =0.7. It is interesting to observe that as low Reynolds number flow stream functions lines are all most filled in the cavity and clockwise rotation will be developed in the bottom left corner as seen in Fig.6 (a). The isotherms are smooth curves which span the entire enclosure and they are symmetric with respect to the vertical center line. increases cold region space dominating inside the cavity, the value of Re =100 has been illustrated in Fig.7 (c).

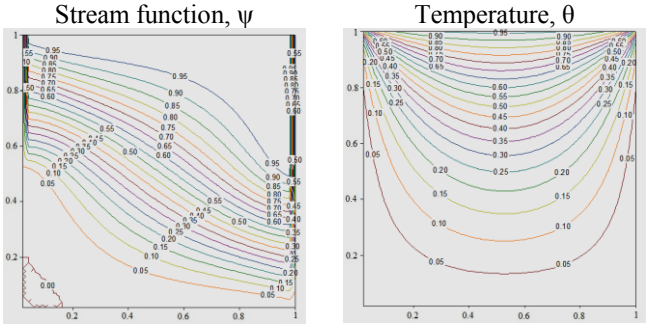

But Fig. 6 (b) and (c) the Re increases bottom left corner circulation strength of stream function increases and stream lines pull up to the top wall. As the value of Re increases, it effect isotherms shift towards the portion of the right wall illustrating that the convection plays a dominant role in the heat transfer and that contrast the cases for fluids with smaller Pr under identical Ri. In the Fig.6 (c) shows that the value of Re increases a small cold region will be developed in the left vertical wall. But Fig. 7 (b) and (c) will seen that value of Prandtl number increases cold region developed inside the cavity will increases, Fig.7 (b) shows the effect at Ri =1, Pr =10 and Re =10, in this case adjacent space at which left side vertical wall are almost cold region. Then the value of Re

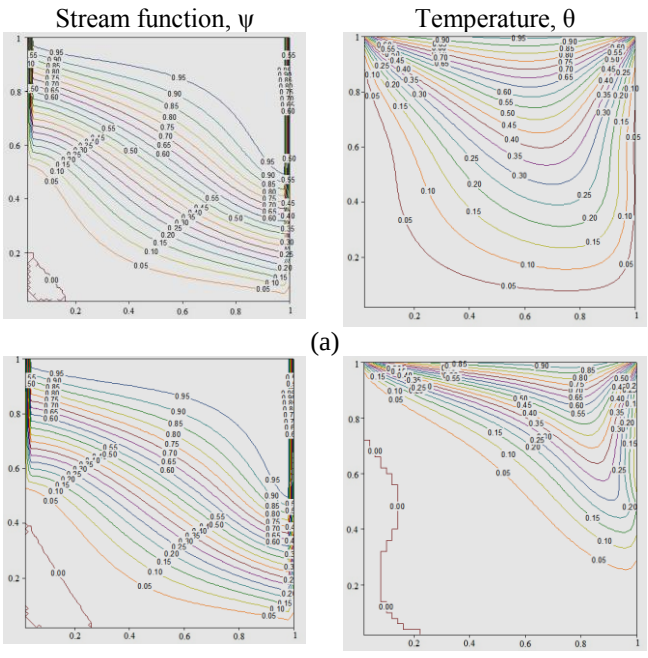

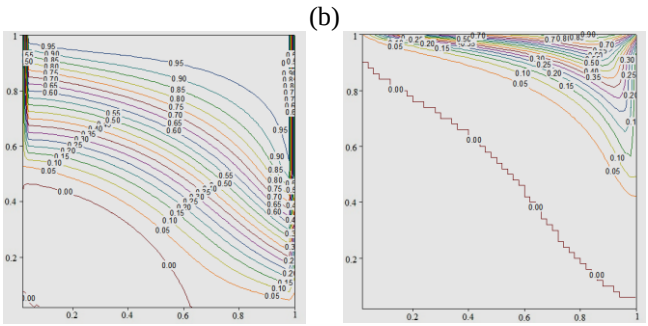

(b)

(c)

Fig.7. Stream function and temperature contours with Pr = 10, Ri =1: (a) Re =1, (b) Re =10, (c) Re =10^2

D. Effect of Prandtl number

Representative streamline plots are displayed in Figure 8 and 9 for different values of Pr at Re= 10 and 100, Ri=1.0. At Ri=1.0, the recirculation region at the lower-left corner is dominated by the adverse pressure gradient effects and the thinning of the thermal boundary layer with increasing Pr does not appear to greatly influence the separation region. As noted earlier, at Pr= 0.7, with increasing values of Re, the flow near the heated surface is accelerated leading to the reduction of the separation along the left end of the heated surface, and resulting in the appearance of the recirculation bubble towards the right end of the heated wall. However, as Pr is increased, the corresponding decrease in the fluid conductivity limits the acceleration of the near hot- wall fluid to a thinner thermal boundary layer region. The thermal boundary decreases in thickness as Pr increases. This is reflected by the denser dust ring of isotherms close to the hot wall as Pr increases. The spread of isotherms at low values of Pr is due to a strong stream wise conduction that decreases the stream wise temperature gradient in the fluid.

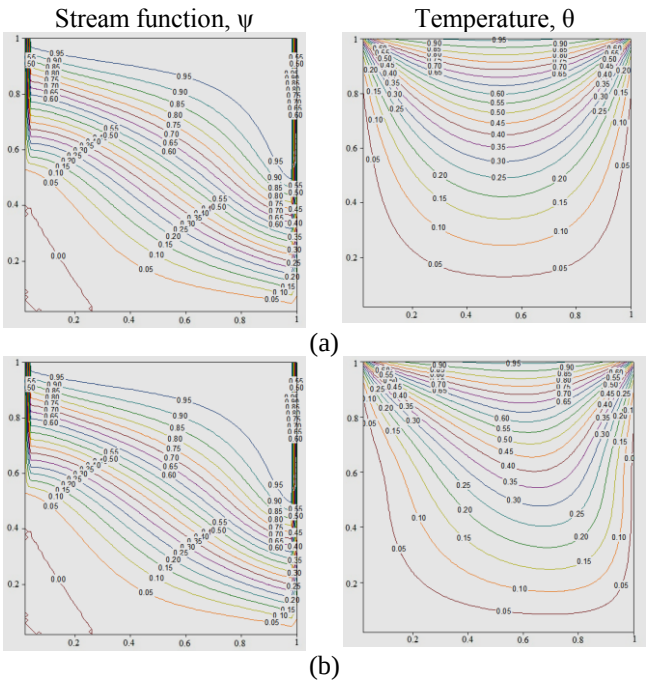

(a)

(b)

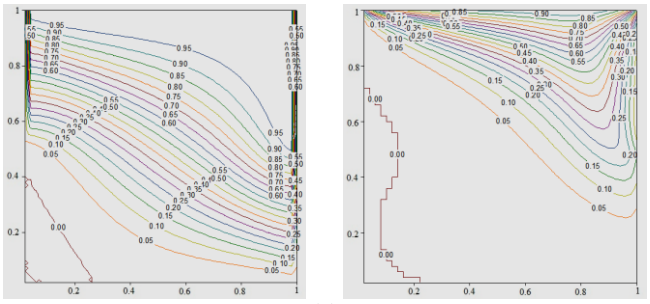

(c)

Fig.8. Stream function and temperature contours with Re =10, Ri =1 :(a) Pr = 0.1, (b) Pr = 0.7, (c) Pr = 1

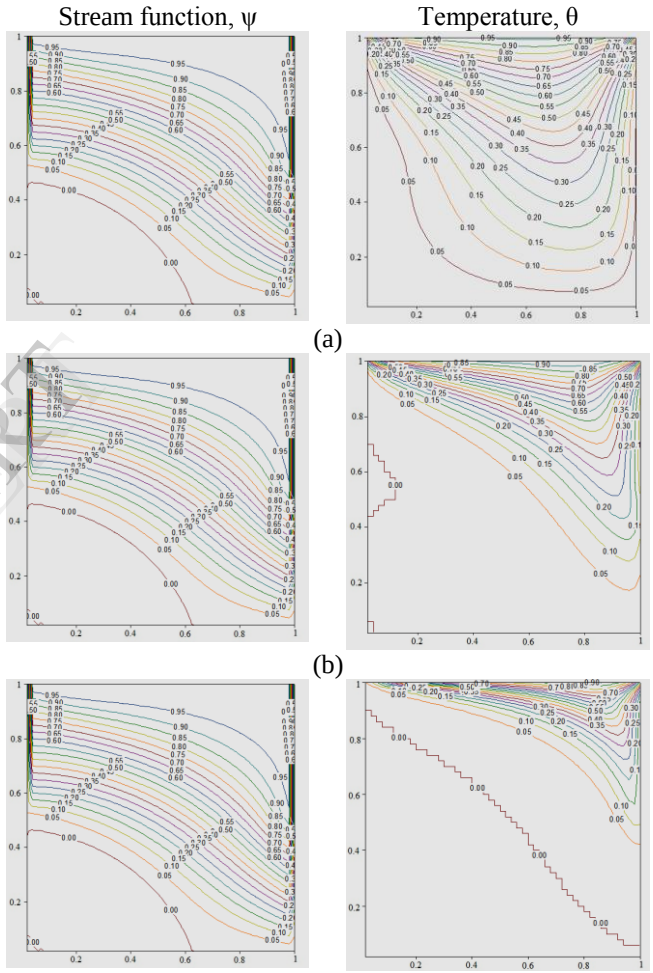

(a)

(b)

(c)

Fig.9. Stream function and temperature contours with Re =100, Ri =1 :(a) Pr = 0.1, (b) Pr = 0.7, (c) Pr = 1

Figs.8 and 9 are interesting to observe that at lower Reynolds number and Prandtl number isothermal contours are smooth and symmetric with vertical center line. As the value of Prandtl number increases thickness of hydrodynamic boundary layer is dominating compared to the thermal boundary layer thickness, then thermal isotherm shifted towers top heated wall. The value of Pr increasing a cold region will be developed at adjacent space to the left vertical wall. Then the value of Re increases, a clockwise circulation or adverse pressure gradient is developed by bottom left of

the enclosure, as it result cold region developed in the cavity. The value of Re and Pr will affect thermal asymmetry in the cavity, higher values of it cold region dominating inside the cavity as seen in Fig.9 (c). The room air conditioning taking based on the cold region in this case heat affected region is reduced.

V. CONCLUSIONS

A numerical investigation on mixed convection in a ventilated enclosure with various boundary conditions was carried out using a finite volume method. The prime objective of the investigation is to study the effect of uniform heating of the top wall, on the flow and heat transfer characteristics due to mixed convection in enclosure. It is evident from Figs. 3-5 for fixed Re and Pr, the strength of circulation increases with the increase in Ri. As Ri increases, the effect of buoyancy increases leading to an increase in the strength of circulation. Due to increase in circulation strength, the isotherms are stretched along the side walls and heat is transferred mostly by convection for higher value of Pr. The effect of Re has also been studied in the present investigation for fixed value of Pr and Ri. It is observed that the effect of natural convection decreases and forced convection increases with the increase of Re. It has also been observed that for higher value of Pr, the effect of heating is more pronounced near the top and right walls as the formation of thermal boundary layers is restricted near the top and right wall for uniform heating cases. The heat transfer rate is very high at the edges of the top wall and it decreases at the center of the cavity.

Laminar convection in a two-dimensional, horizontally driven rectangular enclosure with a prescribed constant temperature heat source mounted on the bottom wall is simulated numerically in this work. Mixed convection arises as the buoyancy-induced cold flow from the source interacts with an externally induced cold air flow. The effects of different ventilation orientations are also described to figure out the best cooling performance. The heat transfer results explain the importance of the non-dimensional parameters like Reynolds number and Richardson number in the natural and mixed convection regime. The effects of these parameters on the flow fields are also investigated. The governing parameter affecting heat transfer is the Richardson number. For Ri > 1, the heat transfer is dominated by natural convection. When Ri < 1, the flow and heat transfer are dominated by forced convection. The mixed regime is obtained when Ri = 1.

ACKNOWLEDGMENT

The authors wish to acknowledge Department of Mechanical Engineering, LBS College of Engineering, Kasaragod, India, for support and technical help throughout this work.

REFERENCES

[1] Burggraf, O.R., Analytical and numerical studies of the structure of steady separated flows, Journal of Fluid Mechanics, 1966, 24, 113-151

[2] O. Botella and R. Peyret., Benchmark spectral results on the lid-driven cavity flow, Computers & Fluids Vol. 27, No. 4, pp. 421-433, 1998

[3] Charles-Henri Bruneau and Mazen Saad., The 2D lid-driven cavity problem revisited, Computers & Fluids 35 (2006) 326–348

[4] Chen, Q., Mayers, C.A., Vander Kooi, J. 1989. "Convective heat transfer in rooms with mixed convection," in: International Seminar on Indoor Air Flow Patterns, University of Liege, Belgium. pp. 69–82.

[5] Spitler, J.D. 1990. "An experimental investigation of air flow and convective heat transfer in enclosures having large ventilation rates," PhD Thesis, University of Illinois at Urbana-Champaign, USA.

[6] Fisher, D.E.1995. "An experimental investigation of mixed convection heat transfer in a rectangular enclosure," PhD Thesis, University of Illinois at Urbana-Champaign, USA

[7] Pavlovic, M. D., Penot, F. 1991. "Experiments in the mixed convection regime in an isothermal open cubic cavity," Experimental Thermal and Fluid Science 4, pp. 648–655.

[8] Du, S-Q., Bilgen, E., Vasseur, P. 1998. "Mixed convection heat transfer in open ended channels with protruding heaters," Heat Mass Transfer 34, pp. 265–270.

[9] Sathe, S.B., Sammakia, B.G. 2000. "A numerical study of the thermal performance of a tape ball grid array (tbga) package," J Electronic Packaging 122, pp. 107–114.

[10] Harman, S.A.,Cole, K.D.2001. "Conjugate heat transfer from a two layer substrate model of a convectively cooled circuit board," J Electronic Packaging. Vol. 123: 156–158

[11] Thrasher, W.W., Fisher, T.S., Torrance, K.E. 2000. "Experiments on chimney-enhanced free convection from pin-fin heat sinks," J Electronic Packaging 122, pp. 350–355.

[12] Jilani, G., Jayaraj,S., Voli, K.K. 2001. "Numerical analysis of free convective flows in partially open enclosure," Heat Mass Transfer. DOI 10.1007/ S002310100251/ online publication, Nov 29.

[13] Ligrani, P.M., Choi, S.1996. "Mixed convection is straight and curved channels with buoyancy orthogonal to the forced flow," Int. J. Heat Mass Transfer Vol. 39(12): 2473-2484.

[14] Hattori,N. 1979. "Combined free and forced convection heat transfer for fully developed laminar flow in horizontal concentric annuli (numerical analysis)," Heat Transfer: Jpn. Res. Vol. 8(4): 27-48.

[15] Karki, K.C., Patankar, S.V. 1989. "Laminar mixed convection in the entrance region of a horizontal annulus," Numer. Heat Transfer 15, pp. 87-99.

[16] Nonio, C., Giudice, S.D. 1996. "Finite element analysis of laminar mixed convection in the entrance region of horizontal annular ducts," Numer. Heat Transfer, Part A 29, pp. 313-330